Machinability of Alloy Steel and Titanium Alloy under Carbon Dioxide Snow, Micro-lubrication and Hybrid Lubro- Cooling

IOP Conf. Series: Materials Science and Engineering **521** (2019) 012003 doi:10.1088/1757-899X/521/1/012003

Machinability of Alloy Steel and Titanium Alloy under Carbon Dioxide Snow, Micro-lubrication and Hybrid Lubro-Cooling

A Iqbal[1], **J Zaini**[1] **and MM Nauman**[1]

[1]Faculty of Integrated Technologies, Universiti Brunei Darussalam, Jln Tungku Link, Gadong BE1410, Brunei Darussalam

asif.asifiqbal@gmail.com

Abstract. Efficient removal of process heat in machining of high-strength alloys is critical to product quality, process cost and productivity. The paper experimentally investigates the effects of employing a cryogenic coolant (CO_2 snow), micro-lubrication and hybridization of the two on the performance measures, such as tool damage, machining forces and specific cutting energy in cutting of two commonly used high-strength alloys, Ti-6Al-4V and 40NiCrMo6. It was found that although the aforementioned cooling approached improved machinability of both the alloys but the titanium based alloy remained more difficult-to-cut than the alloy steel. Hybrid lubro-cooling and CO_2 snow cooling proved to be the most effective options for machining of 40NiCrMo6 and Ti-6Al-4V, respectively.

1. Introduction

Emulsion based flood coolant is in use for decades for dissipation of heat in machining of high-strength alloys but it has some limitations, such as limited cooling capacity, requirement of filtering and pumping, swarf generation and toxicity [1]. Due to extremely low operational temperatures, the cryogenic fluids possess capability of dissipating intense levels of process heat. Furthermore, they do not cause any waste or filtering related problems [2]. Micro-lubrication, also called as minimum quantity of lubrication (MQL), has also been utilized for enhancing machinability[3].

Dhananchezian et al have studied effects of applying liquid nitrogen (LN_2) jet at rake and flank faces through holes provided in the turning insert during the cutting of Ti–6Al–4V [4]. In another work, considerable improvement in tool life, by subduing adhesion, dissolution, and diffusion wear of tool, was reported with the use of LN_2 gas [5]. Improved surface integrity in the machining of a hardened steel is reported when cutting was done under cryogenic environment using PcBN inserts [6]. In another work, CO_2 snow was used in the machining of a high-strength β-titanium alloy (Ti-10V-2Fe-3Al) [7]. The authors have claimed substantial improvement in tool life, mainly due to subdual of notch wear. It was reported that under MQL environment, the major damage modes of coated carbide cutters in milling of an ultra-hard tool steel were suppressed [8]. Hwang et al have reported reduction in cutting forces and work surface roughness in machining of AISI 1045 steel under MQL [9]. It is reported that application of MQL on the tool's rake face in grooving of a β-titanium alloy leads to reduction in tool damage and deflections [10]. Sun et al have compared the effects of using flood coolant and MQL with cryogenic cooling in machining of an $\alpha + \beta$ titanium alloy [11].

In the context, the current work aims to investigate the effects of using CO_2 snow, micro-lubrication and their hybridization on machinability of a commonly used high-strength low-alloy steel (40NiCrMo6) and an $\alpha + \beta$ titanium alloy (Ti-6Al-4V).

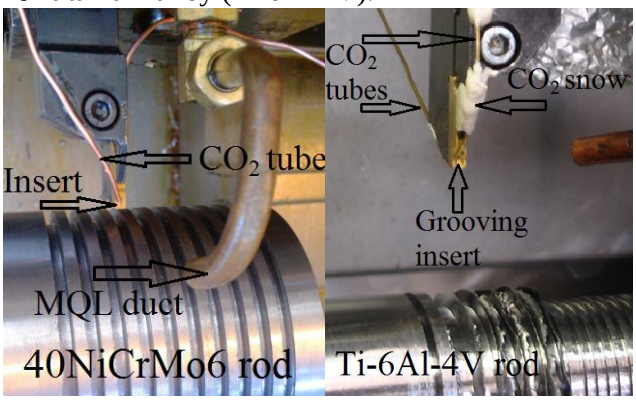

(a) (b)

Figure 1. Experimental setup: (a) alloy steel work rod, MQL duct and CO2 carrying copper tubes; (b) titanium alloy work rod, CO2 carrying copper tubes, and accumulation of CO2 snow in the cutting region.

2. Experimental work

2.1. Predictors

The following predictors were controlled in the experimental runs of a cylindrical grooving process: (a) Work material (40NiCrMo6 and Ti-6Al-4V); (b) Work material's yield strength, R_p (870 MPa and 1,110 MPa); (c) Cooling mode: (1) No coolant (Dry), (2) CO_2 snow on the flank face only (FF-CO_2), (3) CO_2 snow on the rake face only (RF-CO_2), (4) CO_2 snow on the flank face and the rake face simultaneously (FF+RF-CO_2), (5) CO_2 snow on the flank face and MQL on the rake face simultaneously (FF-CO_2, RF-MQL), and (6) CO_2 snow on the rake face and MQL on the flank face simultaneously (RF-CO_2, FF-MQL); and (d) Cutting speed, V_c (80 m/min and 150 m/min).

A multiple-level full-factorial design of experiments was developed that generated 48 runs. The grooving inserts employed were TiN coated tungsten carbide having clearance angle, rake angle and cutting edge's width equal to 12.5º, 1.5º, and 3 mm, respectively. The work material rods were cut into diameters and lengths of 100 mm and 450 mm, respectively. A constant tool's feed rate of 0.12 mm/rev was used in all the experimental runs.

2.2. The setup

All the experimental runs were performed on a CNC lathe having a maximum motor power of 11kW. The micro-lubrication was supplied to the insert's face through a duct by forcing a vegetable oil at a flow rate of 25 mL/hr into the flow of air compressed at 6 bars of pressure. For the application of CO_2 snow at the insert's faces, copper tubes of 1 mm inner diameter were used for transportation of CO_2 gas from a bottle containing the gas. As the compressed gas comes out of the tube, it expands, converts to snow, and produces cooling effect in the surroundings in accordance with the Joule-Thomson phenomenon. Figure 1 presents the experimental setup.

2.3. Responses

The following responses were measured/determined for each experimental run: (a) Maximum width of the flank wear land of the insert after cutting a groove, *VB* (mm); (b) Specific cutting energy, *SCE* (J/mm^3); (c) Average values of the static and dynamic components of: (i) cutting force, F_{c_stat} (N) and F_{c_dyn} (N) and (ii) feed force, F_{c_stat} (N) and F_{c_dyn} (N).

Material removal rate, *MRR* (mm^3/sec), is a productivity measure, which is calculated using the formula, $MRR = 3 \times 0.12 \times (1000 \times V_c/60)$. The numbers "3" and "0.12" are the values of width of cut and feed rate, respectively. The average power consumed by each run was determined using a power

clamp meter, Fluke 345. The *SCE* was obtained by dividing the average cutting power by the corresponding *MRR*. The flank wear was evaluated using a 10× toolmaker's microscope. The machining forces were measured by Kistler Piezoelectric dynamometer 9257B.

Table 1. Experimental results for the 48 runs

No.	Predictors				Responses					
	Work material	R_p (MPa)	Cooling mode	V_c (m/min)	*VB* (mm)	*SCE* (J/mm^3)	F_{c_stat} (N)	F_{c_dyn} (N)	F_{f_stat} (N)	F_{f_dyn} (N)
1	40NiCrMo6	870	Dry	80	0.064	2.744	803	439	524	1009
2	40NiCrMo6	870	Dry	150	0.078	2.218	939	504	606	1032
3	40NiCrMo6	870	FF-CO_2	80	0.049	2.912	803	313	553	887
4	40NiCrMo6	870	FF-CO_2	150	0.060	2.345	982	297	587	974
5	40NiCrMo6	870	RF-CO_2	80	0.051	2.438	750	416	594	961
6	40NiCrMo6	870	RF-CO_2	150	0.066	2.038	824	539	638	1042
7	40NiCrMo6	870	FF+RF-CO_2	80	0.044	2.781	739	457	564	966
8	40NiCrMo6	870	FF+RF-CO_2	150	0.051	2.130	893	515	555	1015
9	40NiCrMo6	870	FF-CO_2, RF-MQL	80	0.039	2.481	679	344	477	657
10	40NiCrMo6	870	FF-CO_2, RF-MQL	150	0.047	2.274	808	361	526	711
11	40NiCrMo6	870	RF-CO_2, FF-MQL	80	0.040	2.388	788	522	601	951
12	40NiCrMo6	870	RF-CO_2, FF-MQL	150	0.054	2.061	897	717	582	993
13	40NiCrMo6	1,100	Dry	80	0.097	3.485	1038	567	663	1132
14	40NiCrMo6	1,100	Dry	150	0.123	2.868	1185	589	698	1241
15	40NiCrMo6	1,100	FF-CO_2	80	0.057	3.487	1021	468	656	1064
16	40NiCrMo6	1,100	FF-CO_2	150	0.071	2.889	1217	438	707	1188
17	40NiCrMo6	1,100	RF-CO_2	80	0.061	2.913	862	624	662	1153
18	40NiCrMo6	1,100	RF-CO_2	150	0.083	2.413	1023	705	691	1286
19	40NiCrMo6	1,100	FF+RF-CO_2	80	0.060	3.344	970	672	677	1154
20	40NiCrMo6	1,100	FF+RF-CO_2	150	0.067	2.645	1106	613	634	1224
21	40NiCrMo6	1,100	FF-CO_2, RF-MQL	80	0.052	2.808	843	568	588	784
22	40NiCrMo6	1,100	FF-CO_2, RF-MQL	150	0.066	2.224	1020	633	630	953
23	40NiCrMo6	1,100	RF-CO_2, FF-MQL	80	0.055	3.065	933	824	776	1138
24	40NiCrMo6	1,100	RF-CO_2, FF-MQL	150	0.072	2.607	1113	868	814	1227
25	Ti-6Al-4V	870	Dry	80	0.108	3.513	748	301	587	419
26	Ti-6Al-4V	870	Dry	150	0.123	3.127	921	383	594	453
27	Ti-6Al-4V	870	FF-CO_2	80	0.072	3.819	694	267	581	559
28	Ti-6Al-4V	870	FF-CO_2	150	0.093	3.315	884	323	581	631
29	Ti-6Al-4V	870	RF-CO_2	80	0.09	3.367	638	488	695	914
30	Ti-6Al-4V	870	RF-CO_2	150	0.108	3.031	801	549	657	987
31	Ti-6Al-4V	870	FF+RF-CO_2	80	0.068	3.062	692	520	558	936
32	Ti-6Al-4V	870	FF+RF-CO_2	150	0.074	2.296	764	543	655	1000
33	Ti-6Al-4V	870	FF-CO_2, RF-MQL	80	0.071	3.571	665	396	501	380
34	Ti-6Al-4V	870	FF-CO_2, RF-MQL	150	0.093	3.280	742	470	615	456
35	Ti-6Al-4V	870	RF-CO_2, FF-MQL	80	0.103	3.010	655	668	637	858
36	Ti-6Al-4V	870	RF-CO_2, FF-MQL	150	0.118	2.414	708	713	675	932
37	Ti-6Al-4V	1,100	Dry	80	0.122	4.429	1223	423	683	603
38	Ti-6Al-4V	1,100	Dry	150	0.139	3.757	1416	535	684	1014
39	Ti-6Al-4V	1,100	FF-CO_2	80	0.075	4.983	1100	588	689	1422
40	Ti-6Al-4V	1,100	FF-CO_2	150	0.099	4.145	1173	644	827	1647
41	Ti-6Al-4V	1,100	RF-CO_2	80	0.105	4.060	903	944	788	2086
42	Ti-6Al-4V	1,100	RF-CO_2	150	0.122	3.595	988	1176	663	2638
43	Ti-6Al-4V	1,100	FF+RF-CO_2	80	0.072	3.806	801	1117	731	2196
44	Ti-6Al-4V	1,100	FF+RF-CO_2	150	0.088	2.839	883	1212	704	2348
45	Ti-6Al-4V	1,100	FF-CO_2, RF-MQL	80	0.075	4.506	1034	588	617	537
46	Ti-6Al-4V	1,100	FF-CO_2, RF-MQL	150	0.105	3.925	1212	651	611	856
47	Ti-6Al-4V	1,100	RF-CO_2, FF-MQL	80	0.109	3.744	869	1008	799	2003
48	Ti-6Al-4V	1,100	RF-CO_2, FF-MQL	150	0.123	3.021	1011	1180	969	2183

3. Experimental results

Table 1 presents the data obtained in respect of the aforementioned response variables. Analysis of Variance (ANOVA) was applied for quantification of the effects of the predictors and their interactions on all the responses. Table 2 presents the ANOVA results in respect of *VB* and *SCE*.

Table 2. Results of ANOVA applied to the data related to *VB* and *SCE*.

Source	Sum of Squares		DoF	Mean Squares		F-value		p-value	
	VB	*SCE*		*VB*	*SCE*	*VB*	*SCE*	*VB*	*SCE*
Work material	0.015	9.24	1	0.015	9.24	872	881	<0.0001	<0.0001
R_p	0.0023	4.65	1	0.0023	4.65	135	443	<0.0001	<0.0001
Cooling mode	0.0094	2.76	5	0.0019	0.55	109	53	<0.0001	<0.0001
V_c	0.0031	3.66	1	0.003	3.66	179	349	<0.0001	<0.0001
Work × R_p	0.0002	0.2	1	0.0002	0.2	14	19	0.0011	0.0003
Work × Cooling	0.0002	1.7	5	0.0003	0.34	20	32	<0.0001	<0.0001

3.1. Tool wear

The ANOVA results in respect of *VB* suggest that work material is the most influential parameter with regard to the tool wear. It's F-value (872) is way too high as compared to those of the other predictors. The titanium alloy is found to be a much more difficult-to-cut material as compared to the high-strength low alloy steel. It suggests that yield strength is not the only work material related parameter that makes a material difficult-to-cut. Beyond material strength, Ti-6Al-4V is also known to have high chemical affinity with various tool materials and low chip-rake contact length. The high levels of yield strength and cutting speed were found to significantly increase the tool wear. The effect of using various cooling modes on tool wear was also found to be significant, which suggests that CO_2 snow based cryogenic cooling possesses potentials to alter the way a cutting tool wears.

Numerical optimization was performed to find out the best cooling option for each of the two work materials for the sake of minimizing tool wear. The optimal cooling modes for cutting 40NiCrMo6 and Ti-6Al-4V were found to be FF-CO_2, RF-MQL and FF+RF-CO_2, respectively. The results suggest that application of CO_2 snow on the tool's flank face causes reduction in the magnitude of flank wear regardless of the work material used. Super-cool jet of CO_2 effectively removes accumulated heat from the cutting edge and vicinity, thereby, suppressing temperature dependent tool wear modes. MQL has shown promising effect only when applied onto the rake face. The *Work* × *Cooling* interaction suggests that the effect of work material on *VB* is most influential when a combination of CO_2 snow and micro-lubrication is used on the opposite tool faces.

The modes of tool wear were analyzed using optical micrography. Two modes of wear, abrasion and wear with various magnitudes of intensity were clearly observed. A complete analysis of the photomicrographs revealed that the adhesive mode of wear was observed in machining of the titanium alloy with its intensity in proportion with the material's yield strength and cutting speed. On the other hand, the intensity of abrasive wear was not dependent upon work material but was in proportion with material's yield strength. Figure 2 presents the micrographs of the selected cutting edges.

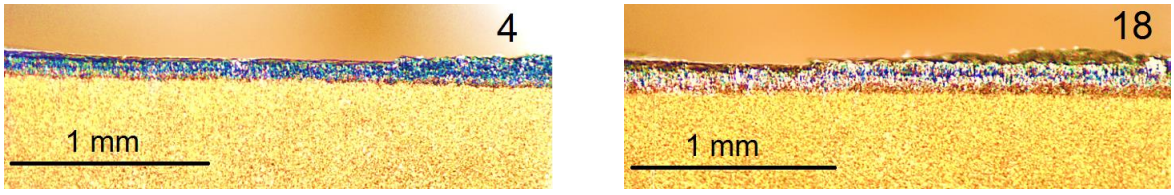

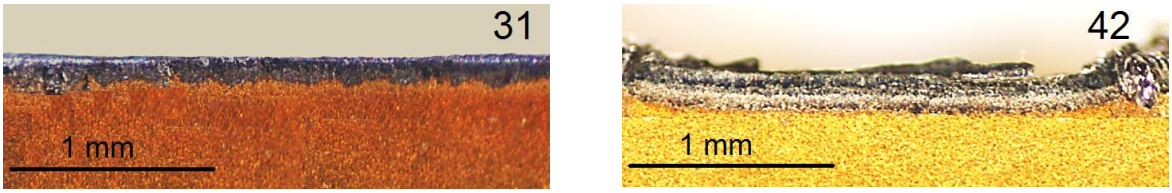

Figure 2. Optical micrographs of the inserts used in the experiments number 4, 18, 31 and 42.

3.2. Specific cutting energy

The ANOVA results in respect of *SCE*, as presented in Table 2, suggest that work material tops the list with respect to strength of effect followed by yield strength, cutting speed and cooling mode. An equally strong Ti-6Al-4V causes more consumption of cutting energy than does the alloy steel because high strength causes accelerated damage to the tool. Cutting with damaged tool geometry demands a high level of cutting force to overcome yield strength of the material, which causes an increase in cutting energy required to cut a unit volume of material. Furthermore, stronger temper of material is cut with a higher level of cutting energy. Cutting speed also has a significant effect on *SCE* with its high level causing reduction in the response's value. Moreover, almost all the cooling modes involving CO_2 snow seem to have a favorable effect on *SCE*. Like tool wear, the optimal cooling modes for the sake of minimizing *SCE* in cutting of 40NiCrMo6 and Ti-6Al-4V are FF-CO_2, RF-MQL and FF+RF-CO_2, respectively. The interaction *Work* × *Cooling* exerts a strong influence on *SCE*. A deeper analysis revealed that the effect of work material's choice is most significant when the applied cooling mode is FF-CO_2, RF-MQL and is least significant when CO_2 is applied on both the faces simultaneously.

3.3. Machining forces

Exceedingly high levels of machining forces, especially in cutting of the stronger temper of the titanium alloy, were observed, as shown in Table 1. ANOVA was applied on the data related to the components of the machining forces. Yield strength was found to be the most influential predictor for all the four force components. Large machining forces were needed to generate the stresses required to overcome the increased level of strength in cutting of the stronger tempers of both the work materials. For most of the cooling modes employed, yield strength has a much more influential effect on the force component when the work material is Ti-6Al-4V.

4. Conclusions

The paper presents an experimental investigation for machinability comparison of Ti-6Al-4V and 40NiCrMo6 under cryogenic and hybrid lubro-cooling environments. Ti-6Al-4V was found to possess poorer machinability than an equally strong high-strength low alloy steel. Though, most of the cryogenic and hybrid lubro-cooling techniques improve the machinability characteristics of both the alloys but the titanium alloy still remains more difficult to cut. Application of CO_2 snow at the flank face of a tool was found to be beneficial for the machinability of both the alloys. Having applied CO_2 snow at the flank face, the option of using micro-lubrication at the rake face proved to be the most suitable one for the machining of 40NiCrMo6. However, the option of applying CO_2 snow on both the tool faces proved to be the most beneficial one for Ti-6Al-4V.

5. References

[1] De Lacalle LL, Angulo C, Lamikiz A and Sanchez JA 2006 *J. Mat. Proc. Technol.* **172** 11
[2] Hong SY 2001 *J. Manuf. Sci. & Eng*. **123** 331
[3] Park KH, Olortegui-Yume J, Yoon MC, and Kwon P 2010 *Int. J Mach. Tools & Manuf*. **50** 824
[4] Dhananchezian M and Kumar MP 2011 *Cryogenics* **51** 34
[5] Venugopal KA, Paul S and Chattopadhyay AB 2007 *Wear* **262** 1071
[6] Umbrello D, Micari F and Jawahir IS 2012 *CIRP Ann. Manuf. Technol*. **61** 103
[7] Machai C and Biermann D 2011 *J. Mat. Proc. Technol.* **211** 1175

[8] Iqbal A, Dar NU, He N, Khan I and Li L. 2009. *Proc. Inst. Mech. Eng. Part B J. Eng. Manuf.* **223** 43.
[9] Hwang YK and Lee CM 2010 J. *Mech. Sci. & Technol*. **24** 1669
[10] Iqbal A, Biermann D, Abbas H, Al-Ghamdi KA and Metzger M 2018 *Int. J. Adv. Manuf. Technol.* DOI: 10.1007/s00170-018-2267-4
[11] Sun Y, Huang B, Puleo DA and Jawahir IS 2015 *Procedia CIRP* **31** 477